PCCP

RSC Publishing

PAPER

View Article Online
View Journal | View Issue

Cite this: *Phys. Chem. Chem. Phys.*, 2013, **15**, 20876

Light intensity dependence of the kinetics of the photocatalytic oxidation of nitrogen(II) oxide at the surface of TiO_2†

Ralf Dillert,*[ab] Astrid Engel,[ab] Julia Große,‡[a] Patrick Lindner[a] and Detlef W. Bahnemann[a]

Received 22nd October 2013,
Accepted 23rd October 2013

DOI: 10.1039/c3cp54469a

www.rsc.org/pccp

Air pollution by nitrogen oxides represents a serious environmental problem in urban areas where numerous sources of these pollutants are concentrated. One approach to reduce the concentration of these air pollutants is their light-induced oxidation in the presence of molecular oxygen and a photocatalytically active building material which uses titanium dioxide as the photocatalyst. Herein, results of an investigation concerning the influence of the photon flux and the pollutant concentration on the rate of the photocatalytic oxidation of nitrogen(II) oxide in the presence of molecular oxygen and UV(A) irradiated titanium dioxide powder are presented. A Langmuir–Hinshelwood-type rate law for the photocatalytic NO oxidation inside the photoreactor comprising four kinetic parameters is derived being suitable to describe the influence of the pollutant concentration and the photon flux on the rate of the photocatalytic oxidation of nitrogen(II) oxide.

Introduction

Air pollution in urban areas, where many sources of polluting organic and inorganic compounds are concentrated, presents a severe risk to the human health.[1–5] Forced by rigorous laws that have been imposed to protect the environment by establishing limiting values for the concentrations of the most frequent air pollutants (*e.g.*, national regulations of European countries on the basis of the EC Directive 2008/50/EC[6]), severe efforts are required to develop technical and non-technical measures to reduce the concentrations of the air pollutants.[7,8] Photocatalytic active building materials such as paints, mortar, glass, tiles, pavement stones, and other concrete products using TiO_2 as the photocatalyst are known to act as sinks for gas phase pollutants. Considered as a passive measure for the removal of air pollutants they have been commercially available for some years. Basic principles and first experiences with their practical application have been reviewed in contributions to journals[9–16] and are summarized in compendia.[17,18]

A very important group of air pollutants are the nitrogen oxides (mainly nitrogen(II) oxide, NO, and nitrogen(IV) oxide, NO_2).[5,19] Therefore, an international standard has been published using NO as the probe molecule to determine the activity of photocatalytic products.[20] The photocatalytic removal of this compound from the gas phase has been intensively studied,[21–64] but still very little is known about the influence of environmental parameters such as temperature, humidity, light intensity, and concentration of other air pollutants on the rate of the photocatalytic reaction. Bengtsson and Castellote[52] have investigated the influence of the NO concentration c_{NO}, the light intensity E, the temperature T, the relative humidity h_r, and the catalyst load l_c on the photocatalytic NO degradation rate at the TiO_2-coated surface of a white mortar in a closed photoreactor. The oxidation kinetics were found to be of first order with the first order rate constant having been approximated by an empirical correlation including all mentioned variables:

$$^{r}r_{NO} = \left(\alpha_1 \exp(\alpha_2/T) + \beta_1 h_r^{\beta_2} + \gamma_1 E^{\gamma_2} + \delta_1 l_c^{\delta_2}\right) c_{NO} \qquad (1)$$

Several authors have used a Langmuir–Hinshelwood-type rate law

$$^{r}r_{NO} = k_{NO}\frac{K_{NO}c_{NO}}{1 + K_{NO}c_{NO}} \qquad (2)$$

to describe the kinetics of the photocatalytic degradation of NO in the gas phase.[53–56,60,62,64] Very recently some papers were

[a] *Institut für Technische Chemie, Leibniz Universität Hannover, Callinstr. 3, 30167 Hannover, Germany*
[b] *Laboratorium für Nano- und Quantenengineering, Leibniz Universität Hannover, Schneiderberg 39, 30167 Hannover, Germany. E-mail: dillert@iftc.uni-hannover.de; Fax: +49 511 7622774; Tel: +49 511 76216039*

† Electronic supplementary information (ESI) available: Details of the experimental set-up and the optimization procedures, and an analysis of kinetic data published in ref. 60. See DOI: 10.1039/c3cp54469a

‡ New address: Advanced Tire Materials, Material & Process Development & Industrialization Tires, Continental Reifen GmbH, Jädekamp 30, 30419 Hannover, Germany.

published discussing the influence of the light intensity and the humidity on the kinetic parameters in eqn (2). Hunger *et al.*[60] have employed this rate law (eqn (2)) to analyze the kinetics of the photocatalytic NO oxidation over TiO_2-containing concrete. They reported an influence of the light intensity E at a constant relative humidity h_r on the rate constant k_{NO} given by $k_{NO} = \alpha_1\left(-1 + \sqrt{1 + \alpha_2 E}\right)$. Despite the fact that their data show a decrease of the kinetic parameter K_{NO} with increasing light intensity E (*cf.* Table 5 and Figure 5 in ref. 60) the authors assumed that K_{NO} is not a function of E ($K_{NO} \neq K_{NO}(E)$). At constant light intensity E the dependence of k_{NO} and K_{NO} on the relative humidity h_r was described by the empirical expressions $k_{NO} = \alpha_3 h_r^{\alpha_4}$ and $K_{NO} = \alpha_5 h_r^{\,2} + \alpha_6 h_r + \alpha_7$, respectively.[60]

Ballari *et al.* investigated the effect of the NO concentration, the light intensity, and the humidity on the rate of the photocatalytic oxidation of nitrogen(II) oxide at concrete pavement stones.[59,61] In a first paper[59] the authors analyzed their experimental data with

$$^{r}r_{NO} = k_{NO}'\left(-1 + \sqrt{1 + \alpha E}\right)\frac{K_{NO}c_{NO}}{1 + K_{NO}c_{NO} + K_{H_2O}c_{H_2O}} \quad (3)$$

whereas in their subsequent work[61]

$$^{r}r_{NO} = k_{NO}'\left(-1 + \sqrt{1 + \alpha E}\right)\frac{K_{NO}c_{NO}}{1 + K_{NO}c_{NO} + K_{NO_2}c_{NO_2} + K_{H_2O}c_{H_2O}} \quad (4)$$

was used considering the competitive adsorption of NO_2 formed during the photocatalytic oxidation of NO.

Very recently, Dillert *et al.*[64] have investigated the photocatalytic oxidation of NO over pure titania samples (Evonik-Degussa Aeroxide® TiO_2 P25) varying the inlet concentration of NO and the light intensity E at constant temperature T and humidity h_a. The results were analyzed in terms of Langmuir–Hinshelwood kinetics, and it was observed that $k_{NO} \approx E^{+(0.86\pm0.14)}$ and $K_{NO} \approx E^{-(0.94\pm0.15)}$. Based on the assumption that the coverage of the photocatalyst surface by the oxidizing species is directly proportional to the flux of the incoming UV(A) photons they derived a Langmuir–Hinshelwood-type rate law with the light-dependent kinetic parameters $k_{NO} = {}^{r}k_{NO}E$ and $K_{NO} = {}^{a}k_{NO}'/({}^{d}k_{NO} + {}^{r}k_{NO}E)$.[64]

Nowadays, numerical methods combining mass transport and surface kinetics are used to predict the performance of photocatalytically active construction materials under environmental conditions.[35,65–70] However, for the precise prediction of the rate of the photocatalytic reaction under consideration a reliable rate law including all relevant environmental variables, *i.e.*, photon flux, humidity, temperature, and pollutant concentrations, is essential but still a desideratum. This work intends to contribute to this task by presenting the derivation of a rate law for the photocatalytic NO removal in air.

Experimental details

The photocatalytic oxidation of NO was measured according to ISO 22197-1,[20] employing a set-up (*cf.* ESI,† Part I) consisting of a test gas supply, a humidifier, three mass flow controllers (Brooks Instrument), a photoreactor (PMMA, borosilicate glass), a light source (Philips, Cleo Compact, λ_{max} = 355 nm, 15 W), and a chemiluminescent NO–NO_x analyser (Horiba APNA 360). For a single degradation test a TiO_2 sample was placed into the photoreactor and covered with a UV(A) transparent glass. The TiO_2 samples were prepared by pressing (1080 kg m^{-2}, 1 min) the photocatalyst Evonik-Degussa Aeroxide® TiO_2 P25 (0.85 g ± 0.02 g) into a rectangular plexiglass folder (height 0.2 cm, width 9.2 cm, length 4.3 cm). The resulting briquettes with a geometric surface area of 3.96×10^{-3} m^2 were irradiated for three days with a UV(A)-lamp (Philips, Cleo Performance UV type 3, λ_{max} = 355 nm, 100 W) at a light intensity of 10 W m^{-2} to remove all organic contaminants possibly adsorbed on their surfaces. At the beginning of each individual test run the NO volume concentration was adjusted within a range from 0.05 to 1.3 ppm ($c_{NO,in}$ = (2–53) × 10^{-6} mol m^{-3}) *via* a bypass mode without photoirradiation. Therefore, an air flow of 3.0 L min^{-1} was combined in a mixing chamber with the needed NO flow ($\dot{V}$ = (3.0–80) × 10^{-3} L min^{-1}; 50 ppm NO in N_2, Linde). Having established the constant volume concentration a dark adsorption of the pollutant on the catalyst surface was accomplished by switching from bypass into reactor mode. After the pollutant volume concentration had risen up to the initial NO concentration again the photoirradiation was performed for 2 h. At the end of the degradation reaction the lamp and the NO-flow were switched off simultaneously. The NO concentration was continuously monitored until it had decreased to 0 ppm.

Most experimental runs were performed with compressed, oil-free air but a few experiments have been performed with molecular nitrogen and oxygen, respectively, being the carrier gas. The light intensity was varied from 0 to 15 W m^{-2} (0–44.8 × 10^{-6} mol photons m^{-2} s^{-1} with λ_{max} = 365 nm) by changing the distance between the UV(A)-lamp and the photoreactor. The light intensity was directly measured before and after the degradation test at three different positions in the photoreactor exactly at the height of the surface of the photocatalyst layer using a radiometer (UV(A)-365, Lutron Electronic) equipped with a sensor collecting the UV(A) irradiation in a range from 320 to 390 nm with a sensitivity maximum at 365 nm. The absolute humidity was calculated from the measurement of the relative humidity and the temperature using a hygrometer (ELV Elektronik AG, TFM 100), which was placed inside the photoreactor. The temperature and the humidity remained constant (T = 25 ± 3 °C, h_r = 50 ± 2%) in all experimental runs.

Results

The photocatalytic degradation of NO on Aeroxide® TiO_2 P25 briquettes was studied in an experimental set-up in accordance with ISO 22197-1 (ref. 20) varying the inlet concentration of NO ($2 \times 10^{-6} \leq c_{NO,in} \leq 53 \times 10^{-6}$ mol m^{-3}) and the incident photon flux ($0 \leq E \leq 44.8 \times 10^{-6}$ mol m^{-2} s^{-1}) at constant temperature (T = 298 K) and humidity (h_a = 11.7 g H_2O m^{-3}). In the absence of UV(A) light $c_{NO,out} = c_{NO,in}$ was found in the

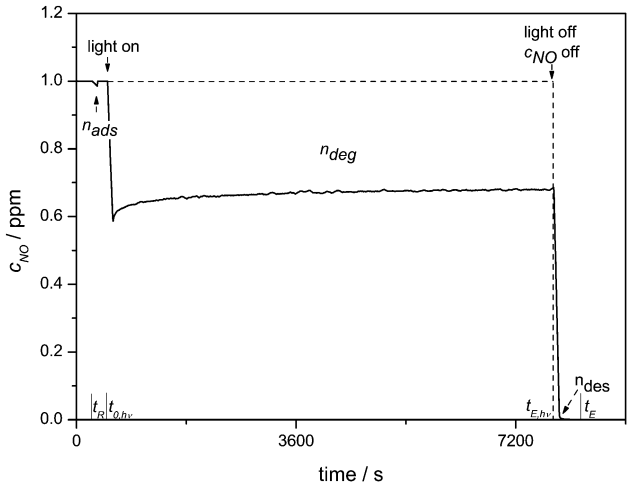

Fig. 1 Time course of the NO concentration at the reactor outlet observed during a typical experimental run with an UV(A) irradiated Aeroxide® TiO_2 P25 sample.

presence as well as in the absence of the photocatalyst, clearly indicating that no dark reactions occur. Within the limits of experimental error no reduction of the NO concentration by homogeneous photoreaction(s) was observed during UV(A) irradiation in the absence of the photocatalyst. Under all investigated experimental conditions a decrease of the NO gas phase concentration was observed under UV(A) irradiation in the presence of the TiO_2 briquettes. The change in the NO concentration at the reactor outlet during a typical experimental run with UV(A) illumination is shown in Fig. 1.

The NO concentration was adjusted to the desired inlet concentration (in Fig. 1: $c_{NO,in}$ = 1 ppm = 41 × 10^{-6} mol m^{-3}) bypassing the photoreactor. When this value was found to be stable the reaction was started by switching the system into the reactor mode without UV(A) irradiation (time t_R). Immediately thereafter, the NO concentration at the reactor outlet was found to decrease, subsequently approaching again the initial inlet concentration. This behaviour can be explained by the displacement of air initially present inside the pipes and the photoreactor and by the dark adsorption of NO followed by the saturation of the surface of the photocatalyst sample and the exposed surface area of the photoreactor and the pipes with adsorbed NO.[64] After the NO concentration was found to be stable for at least five minutes, a shutter between the UV(A) light source and the photoreactor was removed to start the photocatalytic reaction (time $t_{0,h\nu}$). An immediate decrease of the NO concentration was observed. Following two hours of irradiation with UV(A) light, the light-source was switched off and the supply of the NO gas was closed (time $t_{E,h\nu}$). The NO concentration was subsequently recorded until c_{NO} = 0 ppm (time t_E) to allow the calculation of the amount of NO displaced from the reactor after switching off the UV(A) light source, *i.e.*, NO in the gas phase displaced by the air streaming through the reactor and NO desorbing from all surfaces inside the photoreactor and the pipes.

The total amount of the removed NO was calculated using the equation

$$n_{rem} = n_{ads} + n_{deg} - n_{des} \quad (5)$$

with

$$n_{ads} = \frac{p\left(\dot{V}_{air} + \dot{V}_{NO}\right)}{RT} \cdot \sum_{t_R}^{t_{0,h\nu}} \left(c_{NO,in} - c_{NO,out}\right) \cdot \Delta t \quad (6)$$

$$n_{deg} = \frac{p\left(\dot{V}_{air} + \dot{V}_{NO}\right)}{RT} \cdot \sum_{t_{0,h\nu}}^{t_{E,h\nu}} \left(c_{NO,in} - c_{NO,out}\right) \cdot \Delta t \quad (7)$$

$$n_{des} = \frac{p\dot{V}_{air}}{RT} \cdot \sum_{t_{E,h\nu}}^{t_E} c_{NO,out} \cdot \Delta t \quad (8)$$

As it becomes obvious from Fig. 1 the NO concentration was slightly but continuously increasing during the entire duration of the UV(A) irradiation in all experimental runs possibly due to an inhibition of the photocatalyst by the accumulation of photocatalytically generated NO oxidation products at the photocatalyst surface. Since no steady-state concentration of NO at the reactor outlet was reached an average rate of the photocatalytic reaction was calculated by dividing the total removed amount of NO by the geometric photocatalytically active surface area of the sample and the irradiation time:

$${}^{r}r_{NO} = \frac{n_{rem}}{A\left(t_{E,h\nu} - t_{0,h\nu}\right)} \quad (9)$$

In the type of photoreactor employed in this study, *i.e.*, a plug-flow reactor, a gradient of the NO concentration over the photocatalyst surface in the direction of the gas flow is present during UV(A) irradiation. Therefore, an average NO concentration inside the photoreactor was calculated from the measured concentrations:

$$\bar{c}_{NO} = \frac{1}{2N} \sum_{N} \left(c_{NO,in} - c_{NO,out}\right) \quad (10)$$

The photon fluxes, the average NO concentrations inside the photocatalytic reactor, and the average rates of the photocatalytic reactions are tabulated in Table 1. A 3D-plot of the reaction rates *vs.* the mean NO concentrations and the employed light intensities is presented in Fig. 2. It is obvious from the results shown in this figure that in the range of NO concentrations employed in this study ($\bar{c}_{NO} < 52 \times 10^{-6}$ mol m^{-3}) at a high photon flux (E > 40 mol m^{-2} s^{-1}) the reaction rates are increasing nearly linearly with increasing NO concentration inside the photoreactor while at a low photon flux (E < 20 mol m^{-2} s^{-1}) the reaction rates are initially also increasing with increasing NO concentration but finally approaching a limiting value that clearly depends upon the flux of UV photons. This asymptotic behaviour of the graphs observed for low light intensity can easily be explained by assuming a saturation of the TiO_2 surface with adsorbed NO molecules. But then it is to reason that the saturation of the TiO_2 surface by NO molecules is not only depending on the thermodynamic adsorption equilibrium determined by the

Table 1 Reaction rates of the photocatalytic NO oxidation at different UV(A) photon fluxes and NO concentrations

Entry	E (10^{-6} mol m^{-2} s^{-1})	$\bar{c}_{NO}$ (10^{-6} mol m^{-3})	$^{r}r_{NO}$ (10^{-9} mol m^{-2} s^{-1})	Entry	E (10^{-6} mol m^{-2} s^{-1})	$\bar{c}_{NO}$ (10^{-6} mol m^{-3})	$^{r}r_{NO}$ (10^{-9} mol m^{-2} s^{-1})
1	3.15	1.34	11.3	28	28.2	1.18	11.6
2	4.15	3.50	23.6	29	28.6	2.76	26.3
3	4.15	6.59	39.4	30	31.0	5.67	51.7
4	3.26	11.8	73.9	31	30.2	10.8	90.9
5	3.20	18.8	82.0	32	29.0	10.8	124
6	3.20	25.1	104	33	28.6	23.6	169
7	3.20	35.0	82.2	34	29.2	30.6	202
8	3.20	43.8	83.0	35	28.8	38.8	237
9	3.20	51.4	102	36	29.0	46.7	265
10	10.7	1.40	12.7	37	30.4	1.51	16.1
11	10.4	3.49	23.3	38	31.2	2.99	30.8
12	10.5	6.41	41.8	39	31.0	5.59	53.5
13	10.7	10.7	74.8	40	30.9	10.4	100
14	10.7	15.6	92.7	41	31.1	15.1	139
15	10.7	23.6	115	42	32.0	22.1	178
16	10.7	31.1	133	43	31.5	28.2	209
17	10.9	38.2	118	44	31.4	36.1	235
18	10.9	48.1	137	45	30.6	43.1	278
19	21.0	1.55	15.7	46	44.2	1.58	18.2
20	20.8	3.59	32.2	47	47.7	2.91	32.5
21	20.4	5.88	60.9	48	45.5	5.80	63.3
22	20.4	10.6	96.1	49	45.7	9.12	97.1
23	20.2	15.5	135	50	45.6	14.8	144
24	20.7	22.2	170	51	43.8	21.6	192
25	20.4	29.7	193	52	44.1	28.9	230
26	20.4	37.0	222	53	42.7	34.8	282
27	20.4	44.7	227	54	43.9	40.8	325

Note: the standard deviation for $\bar{c}_{NO}$ was smaller than 8% in all experimental runs.

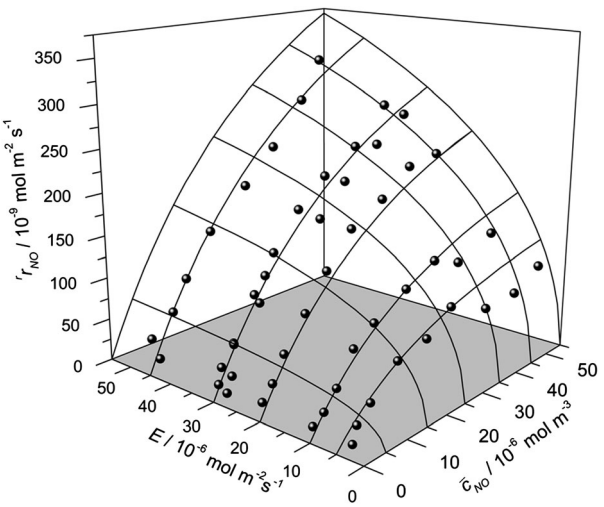

Fig. 2 Dependence of the photocatalytic reaction rate on the mean NO concentration inside the photoreactor and the UV(A) photon flux. The grid was calculated using eqn (19) and the parameters presented in Table 4.

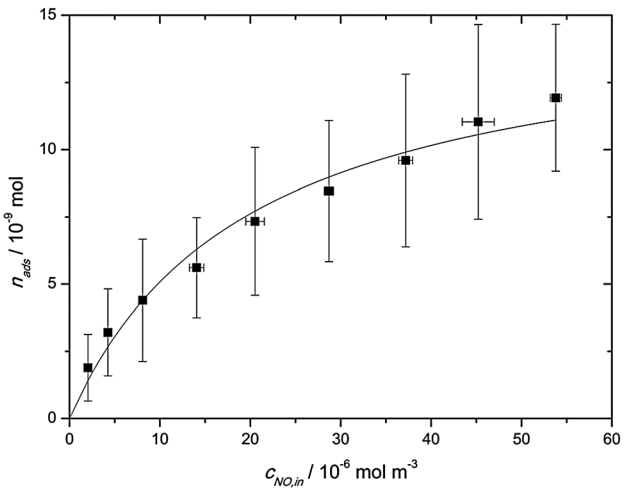

Fig. 3 Langmuir adsorption isotherm of NO on Aeroxide® TiO_2 P25 in the dark. Experimental conditions: T = 298 K, h_r = 50%.

rate constants of the adsorption and desorption but also on the photon flux. The higher the photon flux the lower will be the amount of NO molecules adsorbed on the illuminated photocatalyst surface, *i.e.*, the photo-stationary state surface concentration of NO is clearly smaller than that in the dark. A rate law for the photocatalytic NO oxidation on UV(A) irradiated TiO_2 has to consider this.

To estimate the value of the NO adsorption constant the amount of NO adsorbing in the dark during the experimental run period from t_R to $t_{0,h\nu}$ is plotted *versus* the NO inlet concentrations (Fig. 3). Assuming a Langmuir isotherm the NO adsorption constant and the number of adsorption sites at the photocatalyst surface were estimated by non-linear fitting of the experimental data presented in this figure to be $K_{NO,dark}$ = 5.0×10^4 m^3 mol^{-1} and n_{NO} = 1.5×10^{-8} mol, respectively. In relation to the irradiated geometrical surface area the later value correlates with a number of adsorption sites of 3.8×10^{-6} mol m^{-2}. This value is in a good agreement with the value of 2.7×10^{-6} mol m^{-2} calculated from the data published

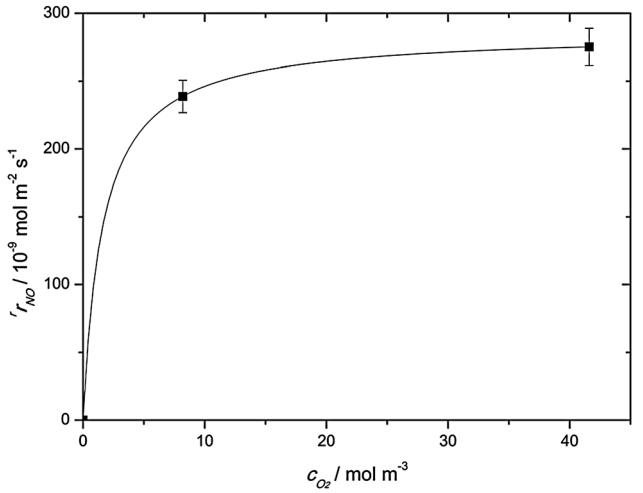

Fig. 4 Dependence of the photocatalytic reaction rate of NO on the oxygen concentration. Experimental conditions: $c_{NO,in}$ = 1 ppm, E = 10 W m^{-2}, T = 298 K, h_r = 50%.

by Hesse and Bredemeyer for the anatase TiO_2 Sachtleben Hombifine N.[71,72]

To obtain information concerning the participation of molecular oxygen in the photocatalytic reaction of NO at the TiO_2 surface, experiments have been performed varying the O_2 concentration in the feed gas by mixing the NO–N_2 test gas with oxygen-free molecular nitrogen, pure molecular oxygen, and air resulting in an NO inlet concentration of 1 ppm. The average reaction rates obtained in this set of experimental runs are plotted *versus* the O_2 inlet concentration in Fig. 4. It becomes obvious from this plot that (a) the presence of molecular oxygen is a prerequisite for the photocatalytic oxidation of NO under the experimental conditions of this study, and (b) that the rate of the photocatalytic oxidation of NO is increasing with increasing oxygen concentration in a Langmuir–Hinshelwood-like fashion. An O_2 adsorption constant of K_{O_2} = 0.62 m^3 mol^{-1} was estimated from the experimental data presented in Fig. 4.

Discussion

The experimental results presented above clearly show that nitrogen(II) oxide is photocatalytically converted on the surface of the Evonik-Degussa Aeroxide® TiO_2 P25 photocatalyst with a reaction rate strongly depending on both the NO concentration in the gas phase above the photocatalyst surface and the photon flux impinging on its surface. During the reaction nitrogen(IV) oxide is released from the photocatalyst surface into the gas phase and nitrite as well as nitrate are formed and accumulated on the TiO_2 sample (data not shown) indicating that the NO conversion is an oxidative degradation process. This is in agreement with published results showing that the final product of the photocatalytic oxidation of NO in the presence of TiO_2 as the photocatalyst is nitric acid (HNO_3) while HNO_2 and NO_2 have been identified as intermediate products adsorbed on the photocatalyst surface and in the gas phase over the photocatalyst. The photocatalytic NO oxidation reaction proceeds consecutively as NO → HNO_2/NO_2^- → NO_2 → HNO_3/NO_3^- at the photocatalyst surface as has been observed by *in situ* Fourier transform infrared spectroscopy and other methods.[22,53] When the UV light is turned on a rapid decrease of the NO concentration is observed evincing a light-induced reaction (Fig. 1). The time course of the NO concentration during irradiation of the photocatalyst (Fig. 1) showing a sudden decrease of the NO concentration immediately after the onset of the UV(A) irradiation followed by a slower increase of the concentration of the probe molecule without reaching a constant value at the reactor outlet can satisfactorily be explained by the dynamic behavior of the plug flow reactor used in this work in combination with mechanistic ideas originally expressed by Devahasdin and co-authors.[53] In the early beginning of the irradiation period no significant gradient of the gas phase NO concentration inside the reactor in the direction of the gas flow is present and the coverage of the surface by adsorbed NO is high over the whole length of the reactor resulting in a high reaction rate over the entire photocatalytically active area. Oxidation products, *i.e.*, HNO_2/NO_2^-, NO_2, and HNO_3/NO_3^-, are formed and accumulated on the surface. The possibility of a photoadsorption process of NO[71–73] during this early stage of the photocatalytic reaction cannot be excluded. After a multiple of the residence time the gradient of the NO concentration in the direction of the gas flow is fully established resulting in a high photocatalytic reaction rate at the entrance region of the photocatalytically active area, where the NO concentration is high, and a lower reaction rate at the outlet, where the NO concentration is decreased. During the entire irradiation time oxidation products are formed which compete with NO for the adsorption sites on the photocatalyst surface thus decreasing the surface concentration of NO and consequently the rate of NO oxidation. It was reported that NO_2 is only weakly adsorbed on TiO_2[74] but that "HNO_3 and related compounds were hardly released" during the photocatalytic oxidation of NO on TiO_2-coated glass.[75] A maximum density of ~2 molecules of HNO_3 nm^{-2} TiO_2 was reported.[74] With the maximum amount of oxidized NO found during this work (n_{rem} = 9.25 × 10^{-6} mol) and the geometric surface area of the sample a maximum density of ~1 molecule of HNO_3 per 1000 nm^2 is calculated to be produced during a single experimental run performed in this work indicating that the TiO_2 surface is far from being saturated by adsorbed HNO_3. It is therefore suggested that a dynamic equilibrium between NO, HNO_2/NO_2^-, and NO_2 is established comprising surface reactions as well as adsorption–desorption equilibria, but that the final oxidation product is continuously accumulated on the photocatalyst surface during the entire experimental run, thus blocking the NO adsorption sites. Hence, no steady-state concentration of NO at the reactor outlet is reached during the entire time of the experimental run (*cf.* Fig. 1).

The nature of the oxidizing species responsible for the photocatalytic oxidation of NO and the resulting reaction pathway was discussed in several publications most of which propose a hydroxyl radical-mediated conversion of NO *via* HNO_2 to yield NO_2, which is subsequently oxidized by the attack of a hydroxyl

Table 2 Proposed photocatalytic reaction pathway of NO with hydroxyl radicals being the oxidizing species

Process	Reaction
Generation of charge carriers	$TiO_2 + h\nu \rightarrow TiO_2(h^+ + e^-)$
Recombination of charge carriers	$TiO_2(h^+ + e^-) \rightarrow TiO_2$
Trapping of charge carriers	$TiO_2(h^+) + H_2O_{ads} \rightarrow TiO_2 + {}^\bullet OH_{ads} + H^+$ $TiO_2(h^+) + OH_{ads}{}^- \rightarrow TiO_2 + {}^\bullet OH_{ads}$ $TiO_2(e^-) + O_{2\,ads} \rightarrow TiO_2 + O_2{}^{\bullet -}$
Oxidation by hydroxyl radicals	$NO_{ads} + {}^\bullet OH_{ads} \rightarrow HNO_{2\,ads}$ $HNO_{2\,ads} + {}^\bullet OH_{ads} \rightarrow NO_{2\,ads} + H_2O$ $NO_{2\,ads} + {}^\bullet OH_{ads} \rightarrow HNO_{3\,ads} \leftrightarrows NO_{3\,ads}{}^- + H^+$
Adsorption–desorption equilibria	$H_2O + site \leftrightarrows H_2O_{ads}$ $O_2 + site \leftrightarrows O_{2\,ads}$ $NO + site \leftrightarrows NO_{ads}$ $HNO_2 + site \leftrightarrows HNO_{2\,ads}$ $NO_2 + site \leftrightarrows NO_{2\,ads}$ $HNO_3 + site \leftrightarrows HNO_{3\,ads}$

radical to the final product HNO_3. The respective photocatalytic oxidation pathway of NO, where water and all nitrogen compounds present at the photocatalyst surface are in equilibrium with the gas phase, is outlined in Table 2.[62–64]

Profound objections have been raised against this pathway by Ohko and co-workers,[24,25,74] who claimed the contribution of a terminal (bridging) oxygen species, $TiO_2(O^\bullet{}_s)$, and oxygen vacancies, $TiO_2(\square)$, at the TiO_2 surface to the photocatalytic NO oxidation. The NO reaction pathway suggested by this group is presented in Table 3.

Table 3 Proposed photocatalytic reaction pathway of NO with lattice oxygen species being the oxidizing species[24,25]

Process	Reaction
Generation of charge carriers	$TiO_2 + h\nu \rightarrow TiO_2(h^+ + e^-)$
Recombination of charge carriers	$TiO_2(h^+ + e^-) \rightarrow TiO_2$
Trapping of charge carriers	$TiO_2(h^+, O_s) \rightarrow TiO_2(O^\bullet{}_s)$ $TiO_2(e^-) + O_{2\,ads} \rightarrow TiO_2 + O_2{}^{\bullet -}{}_{ads}$
Oxidation by holes	$TiO_2(h^+) + NO_{ads} + H_2O_{ads} \rightarrow HNO_{2\,ads} + H^+$ $TiO_2(h^+) + HNO_{2\,ads} \rightarrow NO_{2\,ads} + H^+$ $TiO_2(h^+) + NO_{2\,ads} + H_2O_{ads} \rightarrow HNO_{3\,ads} + H^+$
Oxidation by lattice oxygen radicals	$TiO_2(O^\bullet{}_s) + NO_{ads} + H_2O_{ads} \rightarrow TiO_2(\square) + HNO_{2\,ads} + OH^-{}_{ads}$ $TiO_2(O^\bullet{}_s) + HNO_{2\,ads} \rightarrow TiO_2(O_s) + NO_{2\,ads} + H^+$ $TiO_2(O^\bullet{}_s) + HNO_{2\,ads} \rightarrow TiO_2(\square) + HNO_3{}^-{}_{ads}$ $TiO_2(O^\bullet{}_s) + HNO_3{}^-{}_{ads} \rightarrow TiO_2(O_s) + HNO_{3\,ads}$ $TiO_2(O^\bullet{}_s) + NO_{2\,ads} + H_2O_{ads} \rightarrow TiO_2(\square) + HNO_{3\,ads} + OH^-{}_{ads}$ $TiO_2(O^\bullet{}_s) + NO_{2\,ads} + H_2O_{ads} \rightarrow TiO_2(\square) + NO_3{}^-{}_{ads}$
Reaction of oxygen vaccancies	$TiO_2(\square) + OH^-{}_{ads} \rightarrow TiO_2(O_s) + H^+$

Note: $TiO_2(O_s)$, and $TiO_2(O^\bullet{}_s)$ are terminal (bridging) oxygen species at the TiO_2 surface, and $TiO_2(\square)$ represents bridging oxygen vacancies.

Both suggested mechanisms for the photocatalytic oxidation of NO have the common assumption of a surface reaction between adsorbed NO and one or more adsorbed oxidizing species formed upon the absorption of a photon by the photocatalyst, *i.e.*, a hydroxyl radical ($^\bullet OH_{ads}$), a superoxide radical anion ($O_2{}^{\bullet -}{}_{ads}$), the corresponding hydroperoxyl radical ($HO_2{}^\bullet{}_{ads}$), or an electron-deficient oxygen ($TiO_2(O^\bullet{}_s)$) terminating the TiO_2 surface plane. In both photocatalytic oxidation pathways outlined in Tables 2 and 3 three holes are required to produce the species oxidizing NO to its final reaction product $HNO_3/NO_3{}^-$, and molecular oxygen is assumed to be the principal acceptor for the conduction band electrons generated by the excitation of the TiO_2 photocatalyst. The results obtained while varying the O_2 concentration in the gas phase (Fig. 4) clearly indicate that molecular oxygen is the only suitable electron acceptor in the reaction mixture and its presence is a prerequisite to initiate the photocatalytic oxidation of NO. Therefore, it seems very likely that high amounts of $O_2{}^{\bullet -}/HO_2{}^\bullet$ are produced by the transfer of electrons from the conduction band of the excited semiconductor to molecular oxygen adsorbed on the surface of the photocatalyst. The reaction between NO and $HO_2{}^\bullet$ yielding NO_2 and $^\bullet OH$ ($NO + HO_2{}^\bullet \rightarrow NO_2 + {}^\bullet OH$) is known to occur in the gas phase[75] and it cannot be excluded that the reaction likewise occurs on the TiO_2 surface. The direct formation of HNO_3 initiated by the oxidation of NO by $HO_2{}^\bullet$ ($NO + HO_2{}^\bullet \rightarrow HOONO \rightarrow HNO_3$), which was proposed to occur during the photocatalytic oxidation of NO,[24,26] is known to be only a minor reaction channel of the $NO + HO_2{}^\bullet$ gas phase reaction[76–78] and seems to be unlikely in the photocatalytic reaction. It should be emphasized that only recently experimental evidence for the suggestion that the hydroxyl radical might not even be required for the photocatalytic oxidation of NO and that the superoxide radical anion is to be regarded as the main oxidant was presented by Martinez *et al.*[45]

The possibility of homogeneous reactions in the gas phase between NO and desorbed reactive oxygen species, *e.g.*, $^1O_2$, O_3, $^\bullet OH$, and $HO_2{}^\bullet$, which have been identified over irradiated TiO_2 surfaces[79–86] where they are possibly photocatalytically produced and subsequently desorbed into the gas phase, as well as secondary reactions between nitrogen compounds in the gas phase and/or at the photocatalyst surface, *e.g.*, $NO + NO_2 + H_2O \rightarrow 2HNO_2$ (ref. 29) and $NO + NO_3 \rightarrow 2NO_2$,[24] are usually not considered when the reaction pathway of the photocatalytic NO oxidation is discussed.

The kinetics of the photocatalytic gas phase oxidation of tetrachloro ethene,[87] trichloro ethene,[88] and methanal,[89] to cite only three examples, have been successfully analyzed by deriving rate laws based on the reaction steps of a definite mechanistic scheme. As detailed in the preceding discussion, in the present case the chemical nature of the species responsible for the oxidation of NO and its oxidation products as well as the initial steps of the NO oxidation are still unknown. Therefore, only an empirical rate law based on three fundamental (but of course debatable) assumptions which, however, takes into account the adsorption–desorption equilibria presented in Table 2 can be derived:

Assumption 1: the photocatalytic reaction of nitrogen(II) oxide in the presence of TiO_2 is a bimolecular surface reaction

between adsorbed NO and an oxidizing species with a reaction rate given by

$$ {}^{\mathrm{r}}r_{\mathrm{NO}} = {}^{\mathrm{r}}k_{\mathrm{NO}}\theta_{\mathrm{OX}}\theta_{\mathrm{NO}} \tag{11} $$

where θ_{OX} and θ_{NO} are the fractions of sites occupied by the oxidizing species and by NO, respectively.

Assumption 2: while the chemical nature of the species oxidizing the adsorbed NO molecule is unknown (*vide supra*) it is assumed that the surface coverage by the oxidizing species, θ_{Ox}, is proportional to the number of "free" electrons or holes in the TiO_2. It has been shown[90] that the respective concentrations of both charge carriers are given by equations having the same mathematical form

$$ c_{\text{"free" charge carrier}} = \chi_1\left(-1+\sqrt{1+\chi_2 E}\right) \tag{12} $$

The kinetic parameters χ_1 and χ_2 in eqn (12) are a set of kinetic parameters reflecting the kinetics of the charge carrier recombination in the photocatalyst, of the adsorption of water and molecular oxygen at the photocatalyst surface, and of the interfacial electron transfer, as well as the light absorbing properties of the photocatalyst. Eqn (12) takes into account the known linear and square root dependence of the reaction rate for low and high photon flux, respectively.[90] Rate laws containing the right hand side of this equation have been used to analyze the influence of the photon flux on the photocatalytic degradation of tetrachloro ethene,[87] trichloro ethene,[88] methanal,[89] nitrogen(II) oxide,[60] and nitrogen(II) oxide–nitrogen(IV) oxide mixtures[61] in the gas phase. Therefore, it seems to be reasonable to insert the expression

$$ {}^{\mathrm{r}}k_{\mathrm{NO}}\theta_{\mathrm{OX}} = \chi_1\left(-1+\sqrt{1+\chi_2 E}\right) \tag{13} $$

into eqn (11), where in this particular case the reaction rate constant ${}^{\mathrm{r}}k_{\mathrm{NO}}$ is included in the parameter χ_1.

Assumption 3: following a concept suggested by Ollis[91] the surface concentration of adsorbed NO is obtained by the steady-state approximation

$$ \frac{\mathrm{d}\theta_{\mathrm{NO}}}{\mathrm{d}t} = r_{\mathrm{ads}} - r_{\mathrm{des}} - r_{\mathrm{rem}} \cong 0 \tag{14} $$

assuming that there is no mass transfer limitation and that NO does not compete with other nitrogen-containing compounds for the same adsorption sites but considering the competitive adsorption of H_2O proposed by several researchers.[45,52,53,56,60,63] Consequently, the NO surface concentration is related to the respective gas-phase concentration by

$$ \begin{aligned} \frac{\mathrm{d}\theta_{\mathrm{NO}}}{\mathrm{d}t} &= {}^{\mathrm{a}}k_{\mathrm{NO}}c_{\mathrm{NO}}\left(1-\theta_{\mathrm{H_2O}}-\theta_{\mathrm{NO}}\right) - {}^{\mathrm{d}}k_{\mathrm{NO}}\theta_{\mathrm{NO}} \\ &\quad - \chi_1\left(-1+\sqrt{1+\chi_2 E}\right)\theta_{\mathrm{NO}} \cong 0 \end{aligned} \tag{15} $$

With an additional steady-state condition for water,

$$ \begin{aligned} \frac{\mathrm{d}\theta_{\mathrm{H_2O}}}{\mathrm{d}t} &= r_{\mathrm{ads}} - r_{\mathrm{des}} \\ &= {}^{\mathrm{a}}k_{\mathrm{H_2O}}c_{\mathrm{H_2O}}\left(1-\theta_{\mathrm{H_2O}}-\theta_{\mathrm{NO}}\right) - {}^{\mathrm{d}}k_{\mathrm{H_2O}}\theta_{\mathrm{H_2O}} \cong 0 \end{aligned} \tag{16} $$

the surface coverage by H_2O is given by

$$ \begin{aligned} \theta_{\mathrm{H_2O}} &= (1-\theta_{\mathrm{NO}})\frac{{}^{\mathrm{a}}k_{\mathrm{H_2O}}c_{\mathrm{H_2O}}}{{}^{\mathrm{a}}k_{\mathrm{H_2O}}c_{\mathrm{H_2O}} + {}^{\mathrm{d}}k_{\mathrm{H_2O}}} \\ &= (1-\theta_{\mathrm{NO}})\frac{K_{\mathrm{H_2O}}c_{\mathrm{H_2O}}}{1+K_{\mathrm{H_2O}}c_{\mathrm{H_2O}}} \end{aligned} \tag{17} $$

After inserting eqn (17) into eqn (15) and rearrangement of the resulting equation the coverage of the TiO_2 surface by NO is obtained:

$$ \theta_{\mathrm{NO}} = \frac{\dfrac{{}^{\mathrm{a}}k_{\mathrm{NO}}}{1+K_{\mathrm{H_2O}}c_{\mathrm{H_2O}}}c_{\mathrm{NO}}}{\dfrac{{}^{\mathrm{a}}k_{\mathrm{NO}}}{1+K_{\mathrm{H_2O}}c_{\mathrm{H_2O}}}c_{\mathrm{NO}} + {}^{\mathrm{d}}k_{\mathrm{NO}} + \chi_1\left(-1+\sqrt{1+\chi_2 E}\right)} \tag{18} $$

With these approximations the overall rate of NO elimination in terms of the NO concentration in the gas phase over the photocatalyst is thus given by

$$ \begin{aligned} {}^{\mathrm{r}}r_{\mathrm{NO}} &= \chi_1\left(-1+\sqrt{1+\chi_2 E}\right) \\ &\quad \times \frac{\dfrac{{}^{\mathrm{a}}k_{\mathrm{NO}}}{1+K_{\mathrm{H_2O}}c_{\mathrm{H_2O}}}c_{\mathrm{NO}}}{\dfrac{{}^{\mathrm{a}}k_{\mathrm{NO}}}{1+K_{\mathrm{H_2O}}c_{\mathrm{H_2O}}}c_{\mathrm{NO}} + {}^{\mathrm{d}}k_{\mathrm{NO}} + \chi_1\left(-1+\sqrt{1+\chi_2 E}\right)} \end{aligned} \tag{19} $$

The observed dependence of the photocatalytic reaction rate on the concentration of molecular oxygen (Fig. 4) is easily explained if χ_1 is assumed to be a function of the oxygen concentration given by

$$ \chi_1 = \chi_1{}'\frac{K_{\mathrm{O_2}}c_{\mathrm{O_2}}}{1+K_{\mathrm{O_2}}c_{\mathrm{O_2}}} \tag{20} $$

It was already shown that in the case when $\chi_2 E \ll 1$ the term $\left(-1+\sqrt{1+\chi_2 E}\right)$ in eqn (19) can be approximated by the linear term $0.5\chi_2 E$ of its Taylor series expansion[87] resulting in

$$ \begin{aligned} {}^{\mathrm{r}}r_{\mathrm{NO}} &= \frac{\chi_1\chi_2}{2}E\frac{\dfrac{{}^{\mathrm{a}}k_{\mathrm{NO}}}{1+K_{\mathrm{H_2O}}c_{\mathrm{H_2O}}}c_{\mathrm{NO}}}{\dfrac{{}^{\mathrm{a}}k_{\mathrm{NO}}}{1+K_{\mathrm{H_2O}}c_{\mathrm{H_2O}}}c_{\mathrm{NO}} + {}^{\mathrm{d}}k_{\mathrm{NO}} + \dfrac{\chi_1\chi_2}{2}E} \\ &= \frac{\chi_1\chi_2}{2}E\frac{\dfrac{{}^{\mathrm{a}}k_{\mathrm{NO}}}{\left({}^{\mathrm{d}}k_{\mathrm{NO}}+\dfrac{\chi_1\chi_2}{2}E\right)\left(1+K_{\mathrm{H_2O}}c_{\mathrm{H_2O}}\right)}c_{\mathrm{NO}}}{1+\dfrac{{}^{\mathrm{a}}k_{\mathrm{NO}}}{\left({}^{\mathrm{d}}k_{\mathrm{NO}}+\dfrac{\chi_1\chi_2}{2}E\right)\left(1+K_{\mathrm{H_2O}}c_{\mathrm{H_2O}}\right)}c_{\mathrm{NO}}} \end{aligned} \tag{21} $$

Defining $k_{\mathrm{r}} = \chi_1\chi_2/2$ and ${}^{\mathrm{a}}k_{\mathrm{NO}}{}' = {}^{\mathrm{a}}k_{\mathrm{NO}}/(1+K_{\mathrm{H_2O}}c_{\mathrm{H_2O}})$ the rate law given by eqn (21) reads as

$$ {}^{\mathrm{r}}r_{\mathrm{NO}} = k_{\mathrm{r}}E\frac{\dfrac{{}^{\mathrm{a}}k_{\mathrm{NO}}{}'}{{}^{\mathrm{d}}k_{\mathrm{NO}}+k_{\mathrm{r}}E}c_{\mathrm{NO}}}{1+\dfrac{{}^{\mathrm{a}}k_{\mathrm{NO}}{}'}{{}^{\mathrm{d}}k_{\mathrm{NO}}+k_{\mathrm{r}}E}c_{\mathrm{NO}}} \tag{22} $$

which is equivalent with the rate law recently applied by Dillert *et al.* to analyze a smaller set of the reported NO reaction rates.[64]

After substituting $c_{NO} = \bar{c}_{NO}$ into the eqn (19) the four kinetic parameters χ_1, χ_2, ${}^{a}k_{NO}/(1 + K_{H_2O}c_{H_2O})$, and ${}^{d}k_{NO}$ were obtained from the experimental data presented in Table 1 by mathematical regression routines using a genetic algorithm (GA), and a particle swarm optimizer (PSO). The reason for this approach is that by local, gradient based optimization techniques no reasonable fitting results are obtained. It is assumed that the objective function, in this case the sum of the squared differences between the data predicted by the kinetic model and the experimental data, has several local minima and/or sharp edges and discontinuities. Therefore, it is inevitable to use a global optimization technique like a GA or a PSO to receive optimal or near-optimal parameter values (details of these optimization procedures are presented in the ESI,† Part II).

The results of this non-linear regression of the experimental data are presented in Table 4. In Fig. 5 the calculated rates using eqn (19) and the data given in Table 4 are plotted *versus* the experimental reaction rates revealing a good agreement between the experimental data and the data predicted by the kinetic model.

One assumption made to derive the rate law was that the reaction rate is not limited by mass transport. Therefore, ${}^{a}k_{NO}c_{NO}(1 - \theta_{H_2O} - \theta_{NO}) \geq {}^{r}r_{NO}$ holds and with the lower boundary, given by $(1 - \theta_{H_2O} - \theta_{NO}) = 1$, the rate constant of the NO adsorption can be estimated from the experimental data to be ${}^{a}k_{NO} \geq \left(\frac{{}^{r}r_{NO}}{\bar{c}_{NO}} \cong 5 \times 10^{-3}\ \mathrm{m\ s^{-1}}\right)$. The calculated value $\frac{{}^{a}k_{NO}}{1 + K_{H_2O}c_{H_2O}} = 24.4 \times 10^{-3}\ \mathrm{m\ s^{-1}}$ (Table 4) satisfies this constraint. From the NO adsorption isotherm presented in Fig. 3 it is estimated that $\frac{{}^{a}k_{NO}}{{}^{d}k_{NO}(1 + K_{H_2O}c_{H_2O})} > 5 \times 10^{4}\ \mathrm{m^3\ mol^{-1}}$, while the evaluation of the influence of the NO concentration on the photocatalytic reaction rates at the low photon flux of $\sim 5 \times 10^{-6}$ mol photons $\mathrm{m^{-2}\ s^{-1}}$, where saturation is observed (*cf.* Fig. 2), resulted in $\frac{{}^{a}k_{NO}}{{}^{d}k_{NO}(1 + K_{H_2O}c_{H_2O})} > 10^{5}\ \mathrm{m^3\ mol^{-1}}$. The value $\frac{{}^{a}k_{NO}}{{}^{d}k_{NO}(1 + K_{H_2O}c_{H_2O})} = 4.92 \times 10^{4}\ \mathrm{m^3\ mol^{-1}}$ calculated from the regressed values given in Table 4 is in fairly good agreement with these estimates as well as with published K_{NO} values ($(3.28 \pm 2.06) \times 10^{4}\ \mathrm{m^3\ mol^{-1}}$,[53] $1.27 \times 10^{3}\ \mathrm{m^3\ mol^{-1}}$,[55] $(1.07–1.95) \times 10^{5}\ \mathrm{m^3\ mol^{-1}}$,[60] $8.48 \times 10^{5}\ \mathrm{m^3\ mol^{-1}}$ (ref. 61)) obtained from the analysis of the concentration dependence of the photocatalytic NO oxidation rate. Other related rate laws (see Table 5) were applied to analyze the experimental data presented in Table 1 but were found to be inapplicable, therefore, the suitability of the rate law derived here (eqn (19)) to describe the influence of the NO concentration and the incident photon flux on UV(A) irradiated TiO_2 samples is evident.

It should be noted that the derived rate law (eqn (19)) predicts decreasing rates of the photocatalytic oxidation of NO with increasing concentration of water in the gas phase over a TiO_2 sample. Such a decrease of the reaction rate with increasing concentration of water in the gas phase was in fact reported by several authors.[45,52,53,56,60,63]

The rate law presented in eqn (19) was used to analyse kinetic data recently published by Hunger *et al.*[60] (see ESI,† Part III). A good agreement between experimental and calculated data is observed (ESI,† Fig. S-5) suggesting that the derived rate law is not only valid to describe the photocatalytic oxidation of nitrogen(II) oxide at the surface of the photocatalyst used here (Evonik-Degussa Aeroxide®TiO_2 P25) but also suitable to

Table 4 Results of the non-linear parameter optimization

Kinetic parameter	Unit	Value
χ_1	$\mathrm{mol\ m^{-2}\ s^{-1}}$	3.22×10^{-8}
χ_2	$\mathrm{m^2\ s\ mol^{-1}}$	9.36×10^{6}
$\frac{{}^{a}k_{NO}}{1 + K_{H_2O}c_{H_2O}}$	$\mathrm{m\ s^{-1}}$	2.44×10^{-2}
${}^{d}k_{NO}$	$\mathrm{mol\ m^{-2}\ s^{-1}}$	4.95×10^{-7}

Note: number of data = 54; RSS $< 9.95 \times 10^{-15}$

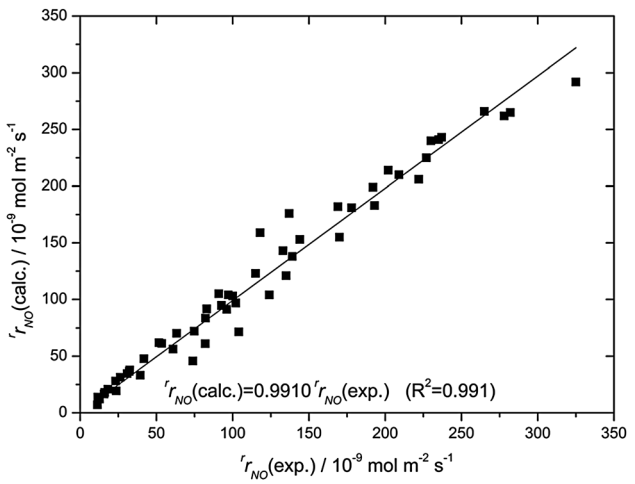

Fig. 5 Plot of the calculated reaction rates *vs.* the experimental reaction rates.

Table 5 Alternative rate laws used to analyze the experimental data given in Table 1

Rate law
$${}^{r}r_{NO} = k_{NO}E\frac{\frac{{}^{a}k_{NO}}{{}^{d}k_{NO}(1 + K_{H_2O}c_{H_2O})}c_{NO}}{1 + \frac{{}^{a}k_{NO}}{{}^{d}k_{NO}(1 + K_{H_2O}c_{H_2O})}c_{NO}}$$
$${}^{r}r_{NO} = k_{NO}\sqrt{E}\frac{\frac{{}^{a}k_{NO}}{{}^{d}k_{NO}(1 + K_{H_2O}c_{H_2O})}c_{NO}}{1 + \frac{{}^{a}k_{NO}}{{}^{d}k_{NO}(1 + K_{H_2O}c_{H_2O})}c_{NO}}$$
$${}^{r}r_{NO} = \chi_1(-1 + \sqrt{1 + \chi_2 E})\frac{\frac{{}^{a}k_{NO}}{{}^{d}k_{NO}(1 + K_{H_2O}c_{H_2O})}c_{NO}}{1 + \frac{{}^{a}k_{NO}}{{}^{d}k_{NO}(1 + K_{H_2O}c_{H_2O})}c_{NO}}$$
$${}^{r}r_{NO} = \chi_1(-1 + \sqrt{1 + \chi_2 E})\frac{\frac{{}^{a}k_{NO}}{1 + K_{H_2O}c_{H_2O}}c_{NO}}{\frac{{}^{a}k_{NO}}{1 + K_{H_2O}c_{H_2O}}c_{NO} + \chi_1(-1 + \sqrt{1 + \chi_2 E})}$$

describe the photocatalytic reaction of this pollutant in the presence of other titanium dioxide samples as well as in the presence of titanium dioxide containing building materials.

Finally, it has to be emphasized again that the rate law derived here and found to be suitable to describe the influence of the pollutant concentration and the photon flux on the rate of the photocatalytic oxidation of nitrogen(II) oxide is an empirical formula not precisely defining the kinetic parameters χ_1 and χ_2. Knowledge concerning the chemical nature of the oxidizing species and additional information about the underlying mechanism of the photocatalytic oxidation reaction(s) of nitrogen(II) oxide as well as about the competitive adsorption between nitrogen(II) oxide and its oxidation products on the photocatalyst surface are highly desired to derive a possibly more accurate rate law.

Conclusions

The rates of the photocatalytic oxidation of nitrogen(II) oxide at different photon fluxes and NO concentrations have been determined. Based on several assumptions concerning the mechanism of the photocatalytic NO oxidation an empirical, Langmuir–Hinshelwood-type rate law was derived comprising four kinetic parameters which were calculated by means of a non-linear optimizing program. A good agreement between the experimental reaction rates and the rates predicted by the derived rate law was observed. Therefore, a prediction of the reaction rates of the photocatalytic NO oxidation on UV(A) irradiated TiO_2 samples at varying nitrogen(II) oxide concentrations and photon fluxes and possibly at varying humidity seems to be feasible.

Nomenclature

A	Geometric photocatalytically active surface area (m^2)
c	Concentration (mol m^{-3} or ppm)
$\bar{c}_{NO}$	Average NO concentration in the photoreactor during irradiation (mol m^{-3})
E	Light intensity (W m^{-2}) or photon flux (mol m^{-2} s^{-1})
h_r, h_a	Relative and absolute humidity ([−] and g m^{-3})
k_{NO}	Kinetic parameter in a Langmuir–Hinshelwood-type rate law (mol m^{-2} s^{-1} or mol m^{-3} s^{-1})
${}^{a}k$, ${}^{a}k'$	Rate constant of the adsorption (m s^{-1})
${}^{d}k$	Rate constant of the desorption (mol m^{-2} s^{-1})
${}^{r}k$	Rate constant of the surface reaction ([−] or mol m^{-2} s^{-1})
$K_{NO,dark}$	Adsorption constant of NO in the dark (m^3 mol^{-1})
K_{H_2O}, K_{O_2}	Adsorption constant of water and molecular oxygen (m^3 mol^{-1})
K_{NO}	Kinetic parameter in a Langmuir–Hinshelwood-type rate law (m^3 mol^{-1})
l_c	Catalyst load
n	Amount (mol)
p	Pressure (Pa)
r	Reaction rate of a surface reaction (mol m^{-2} s^{-1})
${}^{r}r_{NO}$	Average reaction rate of NO (mol m^{-2} s^{-1})
R	Gas constant (J K^{-1} mol^{-1})
R	Correlation coefficient of a regression
t	Time (s)
T	Temperature (K)
$\dot{V}$	Volume flow (m^3 s^{-1})

Greek

α_i, β_i, γ_i, δ_i	Fitting parameters
χ_1, χ_2	Set of kinetic parameters reflecting the charge carrier recombination in the photocatalyst, the adsorption of water and molecular oxygen at the photocatalyst surface, the interfacial electron transfer, and the light absorbing properties of the photocatalyst (mol m^{-2} s^{-1} and m^2 s^{-1} mol^{-1})
θ_{H_2O}, θ_{NO}, θ_{Ox}	Coverage of the photocatalyst surface by H_2O, NO, and the oxidizing species, respectively
λ	Wavelength (nm)

Subscripts

ads	Adsorbed
air	Air
deg	Degraded
des	Desorbed
in	Inlet conditions
irr	Irradiation
max	Maximum
out	Outlet conditions
rem	Removed

Acknowledgements

This work was funded in part by the German Federal Ministry of Education and Research (contract no 03X0069F, "HelioClean – Nanotechnologisch funktionalisierte Baustoffe zur solarkatalytischen Luft- und Oberflächenreinigung"), and by the DFG (BA 1137/8-1).

Notes and references

1 P. J. Lioy and P. G. Georgopoulos, *Environ. Health Perspect.*, 2011, **119**, 1351.
2 M. Hendryx and E. Fedorko, *J. Rural Health*, 2011, **27**, 358.
3 O. Raaschou-Nielsen, Z. J. Andersen, M. Hvidberg, S. S. Jensen, M. Ketzel, M. Sørensen, J. Hansen, S. Loft, K. Overvad and A. Tjønneland, *Environ. Health*, 2011, **10**, 67.
4 A. M. Ragas, R. Oldenkamp, N. Preeker, J. Wernicke and U. Schlink, *Environ. Int.*, 2011, **37**, 872.
5 D. C. Carslaw, S. D. Beevers and M. C. Bell, *Atmos. Environ.*, 2007, **41**, 2073.
6 Directive 2008/50/EC of the European Parliament and of the Council of 21 May 2008 on ambient air quality and cleaner air for Europe, Official Journal of the European Union L 152 (11.06.2008) 1.
7 U. Weiland, *Environ. Impact Assess. Rev.*, 2010, **30**, 211.

8 I. D'Elia, M. Bencardino, L. Ciancarella, M. Contaldi and G. Vialetto, *Atmos. Environ.*, 2009, **43**, 6182.
9 O. Carp, C. L. Huisman and A. Reller, *Progr. Solid State Chem.*, 2004, **32**, 33.
10 A. Fujishima, X. Zhang and D. A. Tryk, *Surf. Sci. Rep.*, 2008, **63**, 515.
11 N. Allen, M. Edge, J. Verran, J. Stratton, J. Maltby and C. Bygott, *Polym. Degrad. Stab.*, 2008, **93**, 1632.
12 J. Chen and C. Poon, *Build. Environ.*, 2009, **44**, 1899.
13 M. Lim, Y. Zhou, L. Wang, V. Rudolph and G. Q. Lu, *Asia–Pac. J. Chem. Eng.*, 2009, **4**, 387.
14 Y. Paz, *Appl. Catal., B*, 2010, **99**, 448.
15 R. de Richter and S. Caillol, *J. Photochem. Photobiol., C*, 2011, **12**, 1.
16 F. Pacheco-Torgal and S. Jalali, *Constr. Build. Mater.*, 2011, **25**, 582.
17 *Photocatalysis, Environment and Construction Materials*, ed. P. Baglioni and L. Cassar, Proceedings of the International RILEM Symposium on Photocatalysis, Environment and Construction Materials -TDP 2007, Florence, Italy, 8–9 October 2007, RILEM Publications, Bagneux, France, 2007.
18 *Applications of titanium dioxide photocatalysis to construction materials*, ed. Y. Ohama and D. van Gemert, State-of-the-Art Report of the RILEM Technical Committee 194-TDP, Springer Netherlands, Dordrecht, 2011.
19 *The European nitrogen assessment. Sources, effects, and policy perspectives*, ed. M. A. Sutton, Cambridge University Press, Cambridge, New York, 2011.
20 ISO 22197-1, Fine ceramics (advanced ceramics, advanced technical ceramics) – Test method for air-purification performance of semiconducting photocatalytic materials – Part 1: Removal of nitric oxide, 2007.
21 T. Ibusuki and K. Takeuchi, *J. Mol. Catal.*, 1994, **88**, 93.
22 I. Nakamura, S. Sugihara and K. Takeuchi, *Chem. Lett.*, 2000, 1276.
23 I. Nakamura, N. Negishi, S. Kutsuna, T. Ihara, S. Sugihara and K. Takeuchi, *J. Mol. Catal. A: Chem.*, 2000, **161**, 205.
24 Y. Ohko, Y. Nakamura, N. Negishi, S. Matsuzawa and K. Takeuchi, *J. Photochem. Photobiol., A*, 2009, **205**, 28.
25 Y. Ohko, Y. Nakamura, N. Negishi, S. Matsuzawa and K. Takeuchi, *Environ. Chem. Lett.*, 2010, **8**, 289.
26 K. Hashimoto, K. Wasada, N. Toukai, H. Kominami and Y. Kera, *J. Photochem. Photobiol., A*, 2000, **136**, 103.
27 H. Ichiura, T. Kitaoka and H. Tanaka, *Chemosphere*, 2003, **51**, 855.
28 Y. M. Lin, Y. H. Tseng, J. H. Huang, C. C. Chao and I. Wang, *Environ. Sci. Technol.*, 2006, **40**, 1616.
29 Y. Ishibai, J. Sato, S. Akita, T. Nishikawa and S. J. Miyagishi, *J. Photochem. Photobiol., A*, 2007, **188**, 106.
30 C. S. Poon and E. Cheung, *Constr. Build. Mater.*, 2007, **21**, 1746.
31 J. Chen, S. Kou and C. Poon, *Build. Environ.*, 2011, **46**, 1827.
32 M. Guo, T. Ling and C. Poon, *Build. Environ.*, 2012, **53**, 1.
33 T. Maggos, J. G. Bartzis, P. Leva and D. Kotzias, *Appl. Phys. A: Mater. Sci. Process.*, 2007, **89**, 81.
34 T. Maggos, J. G. Bartzis, M. Liakou and C. Gobin, *J. Hazard. Mater.*, 2007, **146**, 668.
35 T. Maggos, A. Plassais, J. G. Bartzis, C. Vasilakos, N. Moussiopoulos and L. Bonafous, *Environ. Monit. Assess.*, 2008, **136**, 35.
36 A. G. Kontos, A. Katsanaki, V. Likodimos, T. Maggos, D. Kim, C. Vasilakos, D. D. Dionysiou, P. Schmuki and P. Falaras, *Chem. Eng. J.*, 2012, **179**, 151.
37 J. Hernández-Fernández, A. Aguilar-Elguezabal, S. Castillo, B. Ceron-Ceron, R. D. Arizabalo and M. Moran-Pineda, *Catal. Today*, 2009, **148**, 115.
38 J. Hernández-Fernández, R. Zanella, A. Aguilar-Elguezabal, R. Arizabalo, S. Castillo and M. Moran-Pineda, *Mat. Sci. Eng., B*, 2010, **174**, 13.
39 H. Dylla, M. M. Hassan, M. Schmitt, T. Rupnow and L. N. Mohammad, *J. Mater. Civil Eng.*, 2011, **23**, 1087.
40 C. Águia, J. Ângelo, L. M. Madeira and A. Mendes, *Catal. Today*, 2010, **151**, 77.
41 C. Águia, J. Ângelo, L. M. Madeira and A. Mendes, *Polym. Degrad. Stab.*, 2011, **96**, 898.
42 C. Águia, J. Ângelo, L. M. Madeira and A. Mendes, *J. Environ. Manage.*, 2011, **92**, 1724.
43 Z. Ai, L. Zhu, S. Lee and L. Zhang, *J. Hazard. Mater.*, 2011, **192**, 361.
44 M. Chen and J.-W. Chu, *J. Cleaner Prod.*, 2011, **19**, 1266.
45 T. Martinez, A. Bertron, E. Ringot and G. Escadeillas, *Build. Environ.*, 2011, **46**, 1808.
46 A. Mitsionis, T. Vaimakis, C. Trapalis, N. Todorova, D. Bahnemann and R. Dillert, *Appl. Catal., B*, 2011, **106**, 398.
47 T. Giannakopoulou, N. Todorova, G. Romanos, T. Vaimakis, R. Dillert, D. Bahnemann and C. Trapalis, *Mat. Sci. Eng., B*, 2012, **177**, 1046.
48 G. Guo, Y. Hu, S. Jiang and C. Wei, *J. Hazard. Mater.*, 2012, **223–224**, 39.
49 J. V. Staub de Melo and G. Trichês, *Build. Environ.*, 2012, **49**, 117.
50 B. N. Shelimov, N. N. Tolkachev, G. N. Baeva, A. Y. Stakheev and V. B. Kazanskii, *Kinet. Catal.*, 2011, **52**, 518.
51 Q. Wu, G. Mul and R. van de Krol, *Energy Environ. Sci.*, 2011, **4**, 2140.
52 N. Bengtsson and M. Castellote, *J. Adv. Oxid. Technol.*, 2010, **13**, 341.
53 S. Devahasdin, C. Fan, J. K. Li and D. H. Chen, *J. Photochem. Photobiol., A*, 2003, **156**, 161.
54 H. Wang, Z. Wu, W. Zhao and B. Guan, *Chemosphere*, 2007, **66**, 185.
55 A. Folli, S. B. Campbell, J. A. Anderson and D. E. Macphee, *J. Photochem. Photobiol., A*, 2011, **220**, 85.
56 M. Hunger, G. Hüsken and J. Brouwers, *ZKG Int.*, 2008, **61**(8), 77; M. Hunger, G. Hüsken and J. Brouwers, *ZKG Int.*, 2008, **61**(10), 76; M. Hunger, G. Hüsken and J. Brouwers, *ZKG Int.*, 2009, **62**(2), 63.
57 G. Hüsken, M. Hunger and H. J. H. Brouwers, *Build. Environ.*, 2009, **44**, 2463.
58 G. Hüsken, M. Hunger, M. M. Ballari and H. J. H. Brouwers, The effect of various process conditions on the photocatalytic

degradation of NO, in *Nanotechnology in Construction 3. Proceedings of the NICOM3*, ed. Z. Bittnar, P. J. M. Bartos, J. Němeček, V. Šmilauer and J. Zeman, Springer, Berlin, Heidelberg, 2009, p. 223.

59 M. M. Ballari, M. Hunger, G. Hüsken and H. J. H. Brouwers, Heterogeneous photocatalysis applied to concrete pavement for air remediation, in *Nanotechnology in Construction 3. Proceedings of the NICOM3*, ed. Z. Bittnar, P. J. M. Bartos, J. Němeček, V. Šmilauer and J. Zeman, Springer, Berlin, Heidelberg, 2009, p. 409.

60 M. Hunger, G. Hüsken and J. Brouwers, *Cem. Concr. Res.*, 2010, **49**, 313.

61 M. M. Ballari, M. Hunger, G. Hüsken and H. J. H. Brouwers, *Catal. Today*, 2010, **151**, 71.

62 M. M. Ballari, M. Hunger, G. Hüsken and H. J. H. Brouwers, *Appl. Catal., B*, 2010, **95**, 245.

63 M. M. Ballari, Q. L. Yu and H. J. H. Brouwers, *Catal. Today*, 2011, **161**, 175.

64 R. Dillert, J. Stötzner, A. Engel and D. W. Bahnemann, *J. Hazard. Mater.*, 2012, **211–212**, 240.

65 I. Ossanlis, P. Barmpas and N. Moussiopoulos, The effect of the street canyon length on the street scale flow field and air quality: A numerical study, in *Air Pollution Modeling and Its Application XVII [NATO – Challenges of Modern Society]*, ed. C. Borrego and A.-L. Norman, Springer, New York, NY, 2006, p. 632.

66 A. Plassais, F. Rousseau, E. Eriksson and L. Guillot, Photocatalytic coverings assessment: From canyon street measurements to 3-D modeling, in *Photocatalysis, Environment and Construction Materials. Proceedings of the International RILEM Symposium on Photocatalysis, Environment and Construction Materials-TDP 2007. Florence, Italy, 8–9 October 2007*, ed. P. Baglioni and L. Cassar, RILEM Publications, Bagneux, France, 2007, p. 85.

67 N. Moussiopoulos, P. Barmpas, I. Ossanlis and J. Bartzis, *Environ. Monit. Assess.*, 2008, **13**, 357.

68 M. Bruse and K. Droll, Betonbauteile mit photokatalytisch aktivierten Oberflächen – eine Chance zur Reduzierung des NOx-Gehalts in Städten: Untersuchungsergebnisse und Modellierungsansätze, in *Kolloquium Luftqualität an Straßen 2011. Tagungsbeiträge vom 30. und 31. März 2011*, Bergisch-Gladbach, Bundesanstalt für Straßenwesen 2011, 236.

69 T. Flassak, C. Sörgel, G. Burgeth, W. Duttlinger, M. Maban and J. Kleffmann, Numerische Modellierung des photokatalytischen Stickoxidabbaus durch TiO_2-dotierte Gebäudefassaden, in *Kolloquium Luftqualität an Straßen 2011. Tagungsbeiträge vom 30. und 31. März 2011*, Bergisch-Gladbach, Bundesanstalt für Straßenwesen 2011, 214.

70 L. Neunhäuserer and V. Diegmann, Modellierung des Einflusses photokatalytischer Oberflächen auf die NO_2-Konzentration in der Luft an Verkehrswegen, in *Kolloquium Luftqualität an Straßen 2011. Tagungsbeiträge vom 30. und 31. März 2011*, Bergisch-Gladbach, Bundesanstalt für Straßenwesen 2011, 259.

71 N. Bredemeyer and D. Hesse, *Chem. Eng. Technol.*, 1999, **22**, 580.

72 N. Bredemeyer, S. de Buhr and D. Hesse, *Chem. Eng. Technol.*, 2000, **23**, 527.

73 D. R. Kennedy, M. Ritchie and J. Mackenzie, *Trans. Faraday Soc.*, 1958, **54**, 119.

74 Y. Ohko, Y. Nakamura, A. Fukuda, S. Matsuzawa and K. Takeuchi, *J. Phys. Chem. C*, 2008, **112**, 10502.

75 R. Atkinson, D. L. Baulch, R. A. Cox, J. N. Crowley, R. F. Hampson, R. G. Hynes, M. E. Jenkin, M. J. Rossi and J. Troe, *Atmos. Chem. Phys.*, 2004, **4**, 1461.

76 N. I. Butkovskaya, A. Kukui, N. Pouvesle and G. Le Bras, *J. Phys. Chem. A*, 2005, **109**, 6509.

77 N. Butkovskaya, A. Kukui and G. Le Bras, *J. Phys. Chem. A*, 2007, **111**, 9047.

78 N. Butkovskaya, M.-T. Rayez, J.-C. Rayez, A. Kukui and G. Le Bras, *J. Phys. Chem. A*, 2009, **113**, 11327.

79 Y. Murakami, E. Kenji, A. Y. Nosaka and Y. Nosaka, *J. Phys. Chem. B*, 2006, **110**, 16808.

80 Y. Murakami, K. Endo, I. Ohta, A. Nosaka and Y. Nosaka, *J. Phys. Chem. C*, 2007, **111**, 11339.

81 T. Daimon and Y. Nosaka, *J. Phys. Chem. C*, 2007, **111**, 4420.

82 G. Vincent, A. Aluculesei, A. Parker, C. Fittschen, O. Zahraa and P.-M. Marquaire, *J. Phys. Chem. C*, 2008, **112**, 9115.

83 Y. Nosaka, Surface chemistry of TiO_2 photocatalysis and LIF detection of OH radicals, in *Environmentally benign photocatalysts. Applications of titanium oxide-based materials [Nanostructure Science and Technology]*, ed. M. Anpo and P. V. Kamat, Springer, New York, NY, 2010, p. 205.

84 C. Bahrini, A. Parker, C. Schoemaecker and C. Fittschen, *Appl. Catal., B*, 2010, **99**, 413.

85 J. Thiebaud, F. Thévenet and C. Fittschen, *J. Phys. Chem. C*, 2010, **114**, 3082.

86 M. E. Monge, C. George, B. D'Anna, J.-F. Doussin, A. Jammoul, J. Wang, G. Eyglunent, G. Solignac, V. Daele and A. Mellouki, *J. Am. Chem. Soc.*, 2010, **132**, 8234.

87 G. E. Imoberdorf, H. A. Irazoqui, A. E. Cassano and O. M. Alfano, *Ind. Eng. Chem. Res.*, 2005, **44**, 6075.

88 G. Li Puma, I. Salvado-Estivill, T. N. Obee and S. O. Hay, *Sep. Purif. Technol.*, 2009, **67**, 226.

89 C. Passalía, M. E. Martínez Retamar, O. M. Alfano and R. J. Brandi, *Int. J. Chem. React. Eng.*, 2010, **8**, A 161.

90 S. Upadhya and D. F. Ollis, *J. Adv. Oxid. Technol.*, 1998, **3**, 199.

91 D. F. Ollis, *Top. Catal.*, 2005, **35**, 217.

